Three-Dimensional Flow Model For The Downstream of Kuffa Barrage

Dr. Muhannad J. M. Al-Kizwini*, Dr. Saleh I. Khassaf ⓘ & Majid H. Hobi**

Abstract

The three-dimensional numerical computational fluid dynamics "CFD" computer program "SSIIM" was used to predict the flow field downstream the Kuffa Barrage. It solved the Reynolds-Averaged Navier–Stokes equations in three dimensions to compute the water flow and used the finite-volume method as the discretization scheme. The model was based on a three dimensional, non-orthogonal, structured grid with a non-staggered variable placement. The comparison between filed measurements and numerical results were considered to make the correct decision in this model. The results showed that the maximum velocities were inclined from the river center. The determination coefficients for distribution of velocities ranged from 0.94 to 0.96.

Keywords: Three dimensions, CFD, SSIIM, Kuffa barrage, Reynolds-Averaged Navier–Stokes

أنموذج ثلاثي الابعاد للجريان في مؤخر سدة الكوفة

الخلاصة

في هذه الدراسة تم استخدام أحد برامج حسابات الجريان الحركي للمائع يدعى (SSIIM) الذي يعتمد على حل لمعادلة Reynolds-Averaged Navier–Stokes في الاتجاهات الثلاثة لحسابات الجريان في منطقة المؤخر لسدة الكوفة. اعتمدت هذه المعادلات في مضمونها على استخدام الاحجام المحدودة (Finite Volume) للوصول الى النتائج. الموديل الرياضي في هذه الدراسة كان ثلاثي الابعاد. تم عمل مقارنة بين القراءات الحقلية ونتائج الموديل الرياضي وأعطاء القرار النهائي والصحيح حول الانموذج. توصل البحث الى أنه هنالك علاقة جيدة بين نتائج الموديل الرياضي والقراءات الحقلية وكذلك نبه الموديل الرياضي الى وجود انحراف في توزيعات السرع عن مركزها. معاملات الانحراف لتوزيعات السرع في هذا الموديل تباينت بين 0.94الى 0.96

Introduction

The Navier-Stokes equations for turbulent flow in a general three-dimensional geometry are solved to obtain the water velocity. The k- ε model is used for calculating the turbulent shear stress. A simpler turbulence model can be used. This is specified on the function data in the code of Model (F 24) in the control file of SSIIM program. The Navier-Stokes equations for non-compressible and constant density flow can be modeled as:

$$\frac{\partial U_i}{\partial t} + U_j \frac{\partial U_i}{\partial x_j} = \frac{1}{\rho} \frac{\partial}{\partial x_j}(-P\delta_{ij} - \rho\overline{u_i u_j}) \cdots \quad (1)$$

The left term on the left side of the equation is the transient term. The next term is the convective term. The

* Building and Construction Engineering Department, University of Technology /Baghdad
** Engineering College, University of Kufa / Kufa

first term on the right-hand side is the pressure term. The second term on the right side of the equation is the Reynolds stress term. To evaluate this term, a turbulence model is required.

The equations are discretized with a control-volume approach. An implicit solver is used, also for the multi-block option. The SIMPLE method is the default method used for pressure- correction.

The SIMPLEC method is invoked by the data set in the control file in the program. The power law scheme or the second-order upwind scheme is used in the discretization of the convective terms. This is determined by the values on the data set in the control file. The numerical methods are further described by Patankar (1980), Melaaen (1992) and Olsen (2000).

The default algorithm in SSIIM neglects the transient term. To include this in the calculations the data set in the control file is used. The time step and number of inner iterations are given on this data set. For transient calculations it is possible to give the water levels and discharges as input time series, Zhou Liu, (2001).

2 The turbulent kinetic energy(k)– eddy viscosity (ε) model

The k- ε model calculates the eddy-viscosity as:

$$v_T = c_\mu \frac{k}{\varepsilon^2} \qquad \ldots\ldots\ldots.. (2)$$

k is turbulent kinetic energy constant, defined by:

$$k = \frac{1}{2}\overline{u_i u_i} \qquad \ldots\ldots\ldots (3)$$

k is modeled as:

$$\frac{\partial k}{\partial t} + U_j \frac{\partial k}{\partial x_j} = \frac{\partial}{\partial x_j}\left(\frac{v_T}{\sigma_k}\frac{\partial k}{\partial x_j}\right) + P_k - \varepsilon$$

$$\ldots\ldots\ldots (4)$$

where P_k is given by:

$$P_k = v_T \frac{\partial U_j}{\partial x_i}\left(\frac{\partial U_j}{\partial x_i} + \frac{\partial U_i}{\partial x_j}\right)$$

$$\ldots\ldots\ldots(5)$$

The dissipation of k is denoted , and modeled as:

$$\frac{\partial \varepsilon}{\partial t} + U_j \frac{\partial \varepsilon}{\partial x_j} = \frac{\partial}{\partial x_j}\left(\frac{v_T}{\sigma_k}\frac{\partial \varepsilon}{\partial x_j}\right) + C_{\varepsilon 1}\frac{\varepsilon}{k}P_k + C_{\varepsilon 2}\frac{\varepsilon^2}{k}$$

$$...(6)$$

In the above equations, the c's are different constants. These cannot be changed by the user.

The k- ε model is the default turbulence model in SSIIM.

3 The kinetic energy (k) –Specific dissipation rate (ω) model

In SSIIM, the wall laws for the k-ε model are used also for the k-ω model. This is due to the easier inclusion of roughness.

The k- ω model was developed by Wilcox (2000). It is given by the following equations:

$$v_T = \frac{k}{\omega} \qquad \ldots\ldots.(7)$$

k is turbulent kinetic energy, similar to the k- ε model. k is modelled as:

$$\frac{\partial k}{\partial t} + U_j \frac{\partial k}{\partial x_j} = \frac{\partial}{\partial x_j}\left(\sigma v_T \frac{\partial k}{\partial x_j}\right) + P_k \quad \beta^* k\omega$$

$$\ldots.(8)$$

where P_k is the production of turbulence, similar to the k-epsilon model:

Instead of using the dissipation of k as the second variable, the model uses ω, which is the specific dissipation rate (units seconds[-1]). The equation for is modeled as:

$$\frac{\partial \omega}{\partial t} + U_j \frac{\partial \omega}{\partial x_j} = \frac{\partial}{\partial x_j}\left(\sigma v_T \frac{\partial \omega}{\partial x_j}\right) + \alpha \frac{\omega}{k}P_k - \beta \omega^2$$

The following values and formulas are used for the additional parameters.

Eng. & Tech. Journal, Vol.29, No. 3, 2011

Three-Dimensional Flow Model For The
Downstream of Kuffa Barrage

$$\alpha = \frac{13}{25} \quad \sigma = \frac{1}{2} \quad \beta = \beta_0 f_\beta \quad \beta^* = \beta_0^* f_{\beta^*} \quad \beta_0 = \frac{9}{125} \quad \beta_0^* = \frac{9}{100}$$

$$f_\beta = \frac{1 + 70\chi_\omega^2}{1 + 80\chi_\omega^2} \qquad \chi_\omega = \left| \frac{\Omega_{ij}\Omega_{jk}S_{ki}}{(\beta_0^*\omega)^3} \right|$$

$$f_{\beta^*} = \begin{cases} 1, \chi_k < 0 \\ \frac{1 + 680\chi_k^2}{1 + 400\chi_k^2}, \chi_k > 0 \end{cases} \qquad \chi_k = \frac{1}{\omega^3} \frac{\partial k}{\partial x_j} \frac{\partial \omega}{\partial x_j}$$

$$\Omega_{ij} = \frac{1}{2}\left(\frac{\partial U_i}{\partial x_j} - \frac{\partial U_j}{\partial x_i}\right) \qquad S_{ij} = \frac{1}{2}\left(\frac{\partial U_i}{\partial x_j} + \frac{\partial U_j}{\partial x_i}\right)$$

The k- ω model often gives less turbulent diffusion than the k- ε model. This means it may over predict the size of recirculation zones, whereas the k-ε model often under predicts the recirculation zone length. Wildhagen, J., 2004.

4. Region of study

The region of study is located between Al-Hilla and Al-Najaf city (near AlKifil) (Figure.1). It is located between longitude E 44°,20',45" to E 44°,22',33" and latitude N 32°08'21.3" to N 32°05' 42". In this region the Kuffa barrage is located on the Euphrates river. The reach length is about 3 Km long with an average 200m width. Three bends were located in the reach. They were consedred for the velocity analysis and modeling verification (Figure.2).

5.   Velocity Measurement and Distribution

Twenty cross-sections Figure.3 were considered along the reach. Each cross-section was divided laterally into three equal parts. At each part three vertical measurements along the depth were chosen at 0.2, 0.4, and 0.8 of the total depth as measured upward (Table.1).

A current meter Figure.4 was used to measure the velocity. The number of all measurements were 180 for one outflow discharge from barrage.

Total discharge was determined by summation of partial discharges.

The velocity-area principal was used to compute discharge from current-meter data. This method was useful to verify the barrage outflow discharges which ranged from 30-155m^3/sec during the study period.

6. Represented Domain in CDF

In computation fluid dynamic (CFD) the prototype domain of flow process has to be described in the numerical model. Initially, the grids of model must be close to the real prototype model for better simulation. The convergence of the prototype regime and the numerical model regime is very difficult and complex in this software. This is because SSIIM couldn't represent natural regime easily . To solve the problem, the SSIIM model was connected with other software in order to construct grids. The best solution was to apply a 3-D MAX software. Considering The export and import data files between the two softwares, a technique was used for the first time during this research. The numerical grid consist of 198 rows across the reach with 35 grid cells in each row. Vertically each grid composed of 13 layers, in order to construct geometrically a three dimensional model at the reach, Figures.5 and 6.

7.   Velocity Distribution by Numerical Model

The numerical model presents the distributions of velocities for each location in the reach study, Table.2. In addition the model considered many hydraulic variables such as concentrations of sediments distribution, pressures, Froude Number, viscosity, Epsilon, depth, bed elevations, roughness, eddy viscosity….etc.

After calculation was finished,

secondary flow was observed due to slight bends occurred through the regime in the study reach, as shown in Figure.6. The first one at section i=71, the second at section i=133 and the third one at section i=170. Such behavior of flow led the current to deviate from its primary direction (Figures.7 to Figure.9).

The main secondary motion at the water surface is towards the convex bank. Therefore, the flow elements move downwards reaching the bottom. While flow elements are vectored in wards to the concave bank. Consequently, the flow exhibits a cross-circulation. The combination of this cross-circulation and the major flow direction results into fluid spiral motion.

Due to the centrifugal forces acting on the primary flow causing that the fluid element will follow a curvilinear trajectory. This hydraulic phenomena was difficult to observe practically in site. Therefore, experimental verification for the water flow calculation couldn't be obtained and consequently the numerical model results couldn't be judged precisely. It was necessary to review the literatures in order to verify the numerical model results for this type of flow.

Figures.7 and 9 exhibits the effect of concavity while Figure.8 exhibits the effect of convexity of the banks on the flow regime. the arrows represent the velocity components *v* and *w* in transversal and vertical direction, respectively, and the length of each arrow represent the magnitude of the velocity according to scale in addition to its direction.

In order to present the longitudinal velocity distribution at the chosen cross-sections, the velocities in the vertical layer have been depth averaged, resulting in one representative velocity for each water column. Furthermore, the numerical model uses Cartesian velocity components as dependent variables, so that longitudinal velocity components used in the later comparison must be obtained by transformation to the corresponding directions. Besides the movement of the longitudinal velocity towards downstream also a vertical movement of the maximum velocity was observed. The cross-section at the apexes shows a longitudinal, depth-averaged velocity maximum close to the center of the cross-section. Having a local peak at the close right bank and the beginning of flow toward downstream, as shown in Figure.10A. The Figure shows that the isotaches are compressed, indicating strong velocity gradients. Considering the subsequent cross-sections, the core velocity moves towards the concave bank, while in the vertical direction it drifts towards the center, as can be seen in Figure.10B. In Figure.10 C. the lines of equal velocity are stretched out, indicating the core velocity moves toward the concave bank. Same action was repeated in the downstream bends. Many studies observed the same action in bending regimes. Weiming, (2008).

8. Model Verification

Verification can be defined as a process for assessing the numerical simulation uncertainty and when conditions permit, estimating the sign and magnitude of the numerical simulation error and the uncertainty in that estimated error. (Figure. 12)
However to verify numerical model with prototype the results were

divided into three parts. The first part deals with flow calculation at 0.2 of the depth while the second part deals with at 0.4 of the depth while the third part at 0.8 of the depth as described in Figure.12.

According to the results, Figures.13 indicates that there is fairly good agreement between measured and calculated velocities. With determination coefficient ranged from 0.94 to 0.96. One reason for the deviation between measured and calculated velocities can be due to some lack of accuracy in the measurements of the velocities and to the geometry of the reach. The software, estimate the bed form between the consequent sections according to the data at these sections. This will lead to the geometry to be inexactly modeled. The largest deviations between the measured and modeled velocities were found for velocity distribution at high velocity values, Figure.12. This was due to the effect of the bottom roughness on velocity distribution "Hydraulically rough flow". This phenomena will lead to a high separation layers from the bottom to the surface. This was found to be the main reason behind the disagreement between the measured. The other reason for the deviation between measured and computed velocities was thought to be the size of cell in the model. Reducing the size of the grid cells in areas of small horizontal distance, will probably increase the accuracy in these areas. The decision of number of grid in each direction must be taken with experience in numerical modeling.

Velocity calculations by the SSIIM model at each node were conducted in three dimensions. The more node numbers lead the model to be more time consuming in solving Navier- Stock's equation. The grids are further explained by Olsen (1999). In a structural three dimensional grid, each cell will have three indices, making it easy to identify grid locations

9. Conclusions

This study presents the development and comparison performed in the numerical model SSIIM and a prototype. The study examined the model results with respect to the those observed in the field in order to determine whether the numerical model (SSIIM) is able to predict velocity distribution in the study reach.

According to the results obtained by this study, the following points are concluded:

1. A good relation was observed between the measured and computed values of velocity at the study reach in three dimensions, with determination coefficients ranged from 0.94 to 0.96.

2. In the region study a hydraulic phenomena was observed (secondary flow). Which effect the study reach region hydraulically.

3. The SSIIM is one of the useful tools to predict the velocity distributions in three dimensions which gave good idea about the behavior of the flow velocities.

Notations

Symbol	Symbol Meaning	Unit
U	average velocity	
ρ	Density of water	m/s
P	Pressure	N/m^2
ν_T	Turbulent eddy-viscosity	m^2/s
c,C	constants in k-ε turbulence model	

References:

Eng. & Tech. Journal, Vol.29, No. 3, 2011

**Three-Dimensional Flow Model For The
Downstream of Kuffa Barrage**

[1]Ruether N., Singh J. M., Olsen N. R. B. and Atkinson E., (2005), "3-D Computation Of Sediment Transport At Water Intakes", The Norwegian University of Science and Technology, Trondheim, Norway.

[2]Zhou Liu, (2001), "Sediment Transport", Aalborg University, China.

[3]Olsen, N. R., (2000), " A Three-Dimensional Numerical Model For Simulation Of Sediment Movements In Water Intakes With Multi-block Option", The Norwegian University of Science and Technology.

[4]Wildhagen, J., 2004, "Applied Computational Fluid Dynamics With Sediment Transport In A Sharply Curved Meandering Channel", Norwegian University of Science and Technology (NTNU).Canadian Journal of Botany. 64: 865-874.

Wilcox, D.A. 2000. The effects of deicing salts on vegetation in Pinhook bog, Indiana.

[5]Schlichting, H. (1979). Boundary Layer Theory, 7th ed., New York McGraw-Hill.

[6]Weiming, Wu, (2008), "Computational River Dynamics", National Center for Computational Hydro science and Engineering, University of Mississippi, MS, USA, Taylor & Francis group, London, UK.

[7] Patankar, S. V. (1980) "Numerical Heat Transfer and Fluid Flow",McGraw-Hill Book Company, New York.

[8]Melaaen, M. C. (1992) "Calculation of fluid flows with staggered and nonstaggered curvilinear nonorthogonal grids - the theory", Numerical Heat Transfer, Part B, vol. 21, pp 1- 19.

Eng. & Tech. Journal, Vol.29, No. 3, 2011

Three-Dimensional Flow Model For The Downstream of Kuffa Barrage
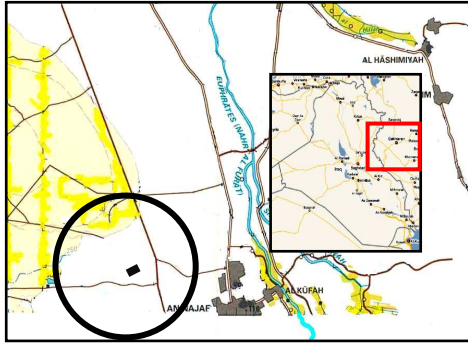
Figure (1) The Map of Region of study

Figure (2) The natural regime of study region, (Google Earth$^{©}$)

Figure (3) The positions of cross-sections (C.S.).

Figure(4): The current mater that used in his study.
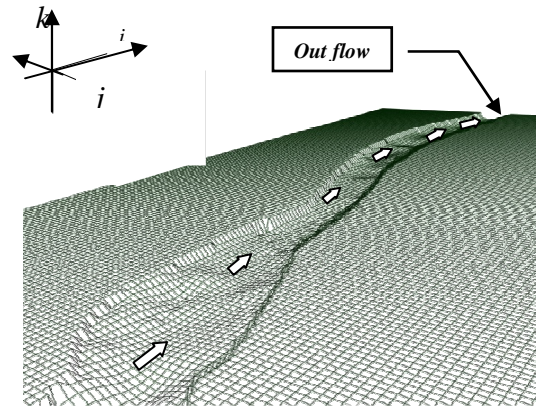
Figure(5) Topography of the reach by the model in three dimensional view
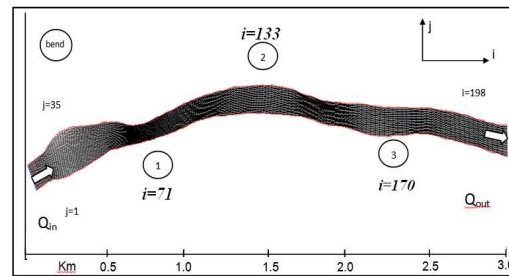
Figure (6) Definition sketch of the mesh(Top view)
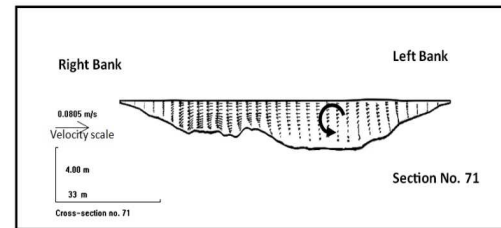
Figure (7) Velocity vectors plot at cross-section bend no. 1
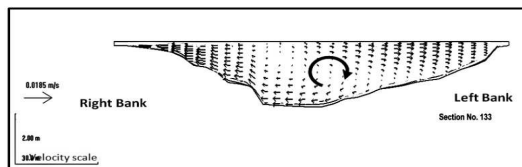
Figure (8) Velocity vectors plot at cross-section bend no. 2
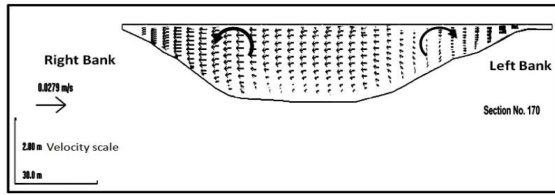
Figure (9) Velocity vectors plot at cross-section bend no. 3
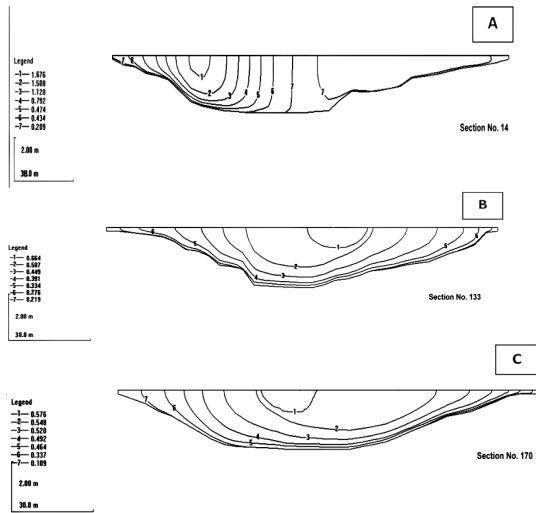
Figure (10) Contour lines for horizontal velocity distribution A at beginning, C at end of region of study
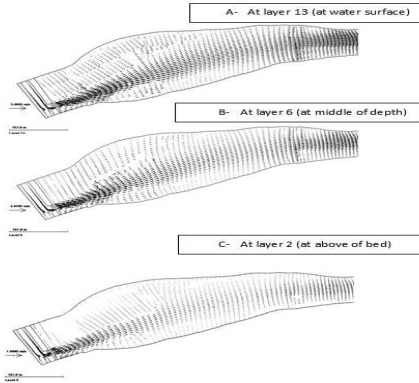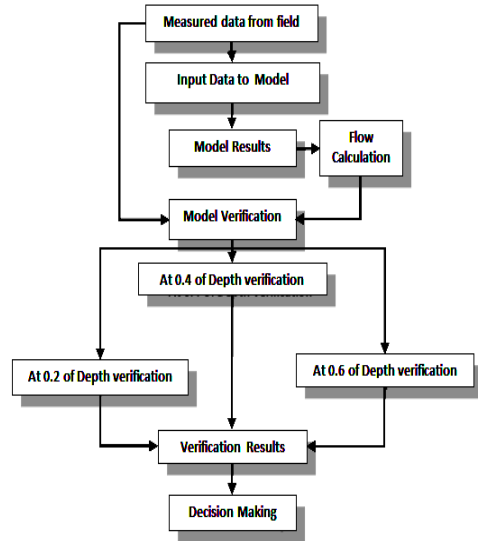
Figure (11) Horizontal (x-y) velocity

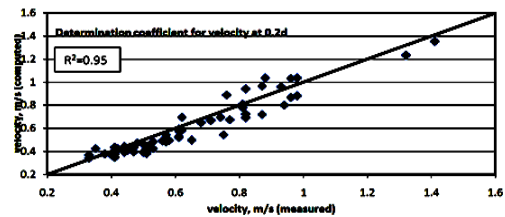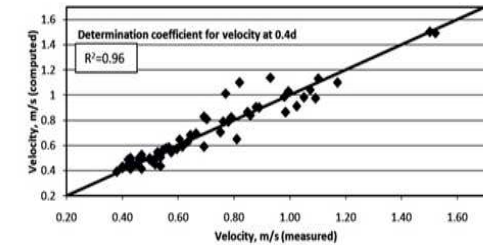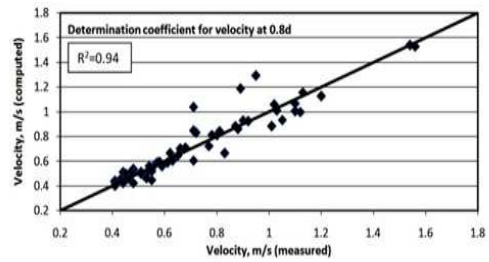Figure. 12: Verification of a numerical model

Figure.13: Determination coefficient for velocity at 0.8d,0.4d and 0.2d between computed and measured for Q=75.62m3/sec